Charge Carrier Interaction with a Purely Electronic Collective Mode: Plasmarons and the Infrared Response of Elemental Bismuth

Riccardo Tediosi,[1] N. P. Armitage,[1,2] E. Giannini,[1] and D. van der Marel[1]

[1]*Département de Physique de la Matière Condensée, Université de Genève, quai Ernest-Ansermet 24, CH1211 Genève 4, Switzerland*
[2]*Department of Physics and Astronomy, The Johns Hopkins University, Baltimore, Maryland 21218, USA*

(Received 17 January 2007; published 6 July 2007)

We present a detailed optical study of single-crystal bismuth using infrared reflectivity and ellipsometry. Large changes in the plasmon frequency are observed as a function of temperature due to charge transfer between hole and electron Fermi pockets. In the optical conductivity, an anomalous temperature dependent midinfrared absorption feature is observed. An extended Drude model analysis reveals that it can be connected to a sharp upturn in the scattering rate, the frequency of which exactly tracks the temperature dependent plasmon frequency. We interpret this absorption and increased scattering as direct optical evidence for a charge carrier interaction with a collective mode of purely electronic origin, here electron-plasmon scattering. The observation of a *plasmaron* as such is made possible only by the unique coincidence of various energy scales and exceptional properties of semimetal bismuth.

DOI: 10.1103/PhysRevLett.99.016406 PACS numbers: 71.45.−d, 78.20.−e, 78.30.−j, 78.40.Kc

Elemental semimetals, such as graphite and bismuth, are materials of much long term interest due to their exceptional properties, including large magnetoresistive and pressure dependent effects [1–3]. In the case of bismuth, these properties derive from its low carrier number ($\approx 10^{-5}$ electrons per atom), reduced effective masses ($\approx 10^{-2}$ electron masses), small Fermi wave vector (≈ 40 nm), and long mean free path (≈ 0.1 mm).

A number of recent results are causing an increased interest in these materials, both from the side of fundamental solid-state physics as well as applications potential. For instance, field dependent crossovers reminiscent of a metal-insulator transition have been observed in both graphite and bismuth [4,5]. Isolated single layers of graphene have been shown to have novel transport properties and an anomalous quantization of the quantum Hall effect resulting from their exceptional zero mass Dirac cone dispersion relation [6,7]. Moreover, there continues to be interest in bismuth for quantum confinement studies [8]. On the technical side, advances in film growth [9], anomalously long spin diffusion lengths, and very large magnetoresistive response make bismuth useful for possible incorporation in nanomagnetometers, magnetooptical devices, and spintronics applications [10,11].

In principle, transport phenomena in bismuth should be well described by the conventional metals theory, but due to the exceptionally low Fermi energy, effective masses and charge densities there are substantial departures from standard metallic behavior. Moreover, the material's very low carrier density opens up the possibility for novel plasmonic effects and strong electron-electron interactions due to the relative scales between potential and kinetic energy at low charge densities [12].

In this Letter, we present detailed temperature dependent optical measurements over the full optical range from far-infrared (FIR) to UV of single-crystal bismuth. We observe a narrow Drude peak and a plasmon energy consistent with the low carrier number. Large changes in the plasmon frequency are observed as a function of temperature. We find an anomalous midinfrared absorption in the real part of the conductivity. An extended Drude model analysis reveals that the scattering rate has an abrupt onset at a temperature-dependent energy scale which is found to be almost exactly coincident with the independently measured plasmon energy. This provides direct optical evidence of a composite particles consisting of conduction electrons coupled to plasmons—i.e., *plasmarons*. As this coupling can feedback on the low energy physics of such systems, our results show that these collective effects must also be considered for correlations in semimetals.

Single-crystal bismuth was grown by a modified Bridgman-Stockbarger technique in a vertical three-zone furnace. A silica tube was filled with ~5 g of 99.999% pure Bi powder (Cerac) and sealed under vacuum. The ampoule was annealed above the melting point of Bi ($T_m = 271.4\,^{\circ}\mathrm{C}$) for 10 hours before decreasing the temperature at a rate of $30\,^{\circ}\mathrm{C/h}$, while keeping a temperature gradient of 10–15 $^{\circ}\mathrm{C/cm}$. The crystals were cleaved from the as-grown boule along a plane perpendicular to the trigonal direction [001] at LN_2 temperatures. X-ray powder diffraction revealed that the mirrorlike cleavage surfaces were [110] planes perpendicular to the trigonal axis which were subsequently used as reflecting surfaces for optical experiments.

We measured the dc resistivity and optical spectra in the frequency range from 50 cm^{-1} (6.2 meV) to 30000 cm^{-1} (3.8 eV) combining quasinormal incidence ($\theta_{\mathrm{inc}} = 11°$) infrared (IR) reflectivity via Fourier transform spectroscopy, and ellipsometry in the visible-UV energy range. The absolute value of the reflectivity $R(\omega, T)$ was measured by

calibrating the signal against a reference gold layer evaporated *in situ* on the sample surface. In the relevant spectral range, our measurements are very bulk sensitive with probing depth of a few microns. A beam splitter absorption at 380 cm^{-1} leaves a weak artifact visible in Fig. 1 that does not reflect an intrinsic feature of the sample. Since it does not affect our conclusions either way, this artifact has been removed from the data used to generate the plots in subsequent figures.

In Fig. 1, the reflectivity is presented for five selected temperatures in the far-infrared spectral range. A shift of the reflectivity edge from around 333 cm^{-1} at room temperature to a value of 164 cm^{-1} at 20 K indicates a strong reduction of the plasmon frequency with cooling. This derives from a change in density due to thermal charge transfer from electron to hole pockets. Carrier densities are consistent with those extracted via transport measurements [13].

The ellipsometry and IR data were combined using a Kramers-Kronig consistent variational fitting procedure [14]. This allows the extraction of all the significant frequency and temperature dependent optical properties like, for instance, the complex conductivity $\hat{\sigma}(\omega, T) = \sigma_1 + i\sigma_2$. The extended frequency range and ellipsometry used in our experiment allows us to extract more accurate parameter values from the subsequent analysis than what has been reported in previous work [15] where just the infrared spectral range was analyzed.

In Fig. 2(a), the optical conductivity $\sigma_1(\omega)$ is presented for corresponding data of Fig. 1 in the FIR-MIR range. The plot reveals two main features developing with decreasing temperature. The first is a narrowing of the Drude peak from an half-width-half-maximum value of 42.3 cm^{-1} at room temperature down to a value of 3.3 cm^{-1} at 20 K. Additionally, we observe a dramatic appearance and strengthening of an absorption centered around 700 cm^{-1} and characterized by an onset approximately around 350 cm^{-1} at room temperature which appears to shift downward as the temperature is lowered. In the inset to Fig. 2, the conductivity is presented over the full measurement range at room temperature; a prominent peak is evident in the figure centered around 5500 cm^{-1} whose energy and temperature dependence are compatible with the direct interband transition at the L-symmetry point.

While the narrowing of the Drude peak is typical behavior for a metal whose dc conductivity increases at lower temperatures as a consequence of the reduction of the scattering processes, the appearance of an MIR absorption is unusual. In fact, a closer look shows an even more interesting aspect, as shown in Fig. 2(b) where we plot a greatly expanded view of the related quantity, the imaginary dielectric constant $\epsilon_2 = 4\pi\sigma_1/\omega$; the low energy onset of this MIR absorption feature is preceded by a small, but distinct and temperature dependent *prepeak* absorption. This prepeak is a robust feature, which we have observed in even poly-crystalline samples. We note that this absorption is also readily visible in the raw reflectivity data itself. For instance, it is apparent in the 20 K curve where it appears as an inflection point slightly above the sharp reflectivity minimum.

In a previous study, the MIR absorption has been assigned to the threshold for direct interband transitions at

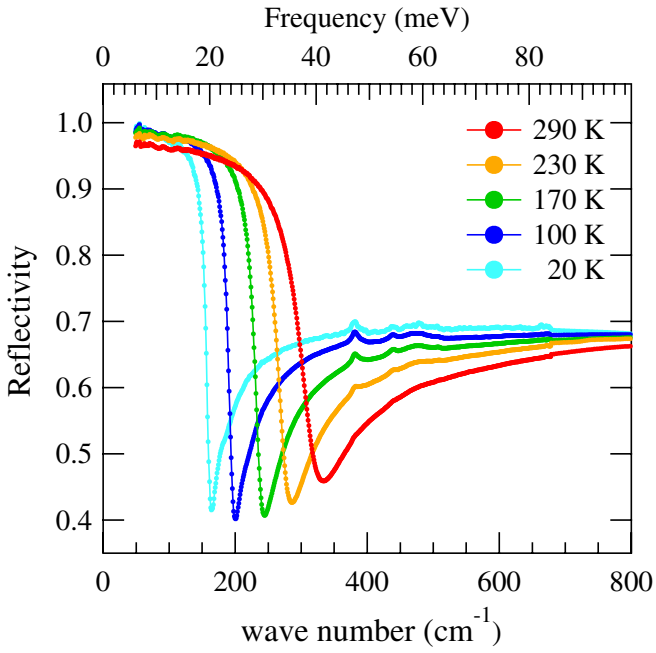

FIG. 1 (color online). Single-crystal bismuth reflectivity vs wave number ($\omega/2\pi c$) for temperatures from 290 to 20 K. The pronounced shifting of the minimum in the range 180–350 cm^{-1} represents the position of the screened plasma frequency ω_p^*.

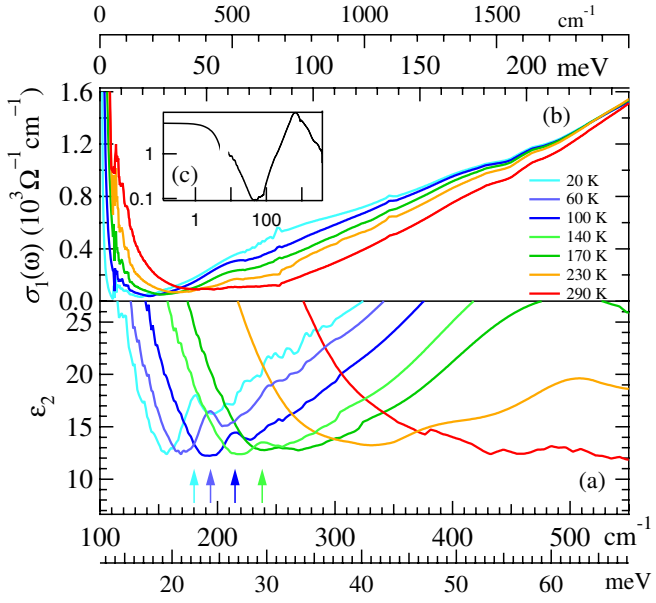

FIG. 2 (color online). (a) Optical conductivity derived from Kramer-Kronig analysis for selected temperatures. (b) The imaginary dielectric constant ϵ_2 over a much smaller energy range that emphasizes the remarkable prepeak structure. (c) Log-Log scale plot of $\sigma_1(\omega)$ for $T = 290$ K, units are meV.

the L point [15]. Certainly such transitions play a role in part of this energy range, but the energy scale of the onset and prepeak are not quite right for them to be the entire contribution. The low temperature interband gap is 13.7 meV [3] and combined with an L point Fermi energy E_F, gives a minimum threshold for direct absorption of $E_c + 2E_F$ of 67.1 meV (540 cm^{-1}), which is much bigger than the onset. The discrepancy even increases at low temperature where the onset falls to 125 cm^{-1}.

In Fig. 3, we analyze the complex conductivity data in terms of the extended Drude model [16], providing the frequency dependent scattering rate $\tau^{-1}(\omega)$ and effective mass $m^*(\omega)$

$$\omega m^*(\omega)/m + i\tau^{-1}(\omega) = (\omega_p^2/\omega)[\varepsilon_\infty - \varepsilon(\omega)]^{-1} \quad (1)$$

where ω_p is the total *intraband* plasma frequency (not to be confused with the *plasmon* frequency ω_p^*), and ε_∞ represents the temperature dependent interband contribution to the dielectric constant. These frequency dependent mass and scattering rate represents the complex self-energy of an optically excited electron-hole pair and reveals rather directly the effect of coupling of the conduction electrons to the (typically bosonic) inelastic scattering channels. We emphasize that the extended Drude model is meaningful only below the onset of interband transitions. One can see in the normalized quantities presented in Fig. 3 that the data are relatively well described at the lowest frequencies within the usual Drude framework where the scattering rates and masses are frequency independent over roughly the same frequency interval. However, we observe a sharp onset in the scattering rate at a well-defined temperature dependent energy scale. This reflects the MIR absorption pointed out previously.

As noted earlier, according to band structure parameters [17], the position of the scattering onset ω_τ is too low to derive from a direct interband process. We observe that the temperature dependence of this absorption's onset and prepeak is reminiscent of the large temperature dependence of the screened plasma frequency itself. In fact, it almost exactly tracks the independently measured plasmon frequency as a function of temperature, as shown in the parametric plot Fig. 4(a) where we plot the frequency of this onset in the $\varepsilon_2(\omega)$ function ω_τ vs ω_p^* as defined by the zero crossing of the experimental $\varepsilon_1(\omega)$, and the onset is defined by the energy position of the prepeak's half maximum on its low frequency side. Based on this parametric plot in Fig. 4, we can conclusively identify the plasmon frequency (which changes a factor of 2 as a function of temperature) as setting the energy scale for the observed absorption process.

Because of its longitudinal character, direct excitation of a plasmon by an incident electromagnetic wave is generally not possible. However, a number of scenarios may exist to induce an electron-plasmon coupling effect. Previously, an explanation for the appearance of the MIR absorption has been given in terms of an impurity-mediated electron-plasmon coupling [18–21]. It was proposed that enhanced electron-charged impurity scattering is found near ω_p^* due to the divergence of $1/\epsilon$. Although our data are in qualitative agreement with such a scenario, the model used by Gerlach *et al.* [19] has a quantitative

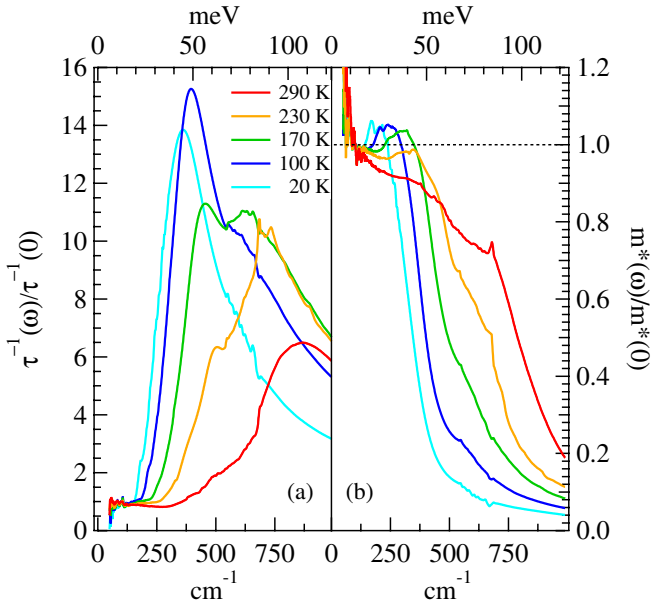

FIG. 3 (color online). Frequency dependent scattering rate (a) and effective mass (b) normalized to their dc values, calculated from the optical data with Eq. (1) using ε_∞ smoothly varying between 134 (20 K) to 108 (290 K). An approximately frequency independent region is interrupted by a sharp onset in scattering and peak in the mass ratio.

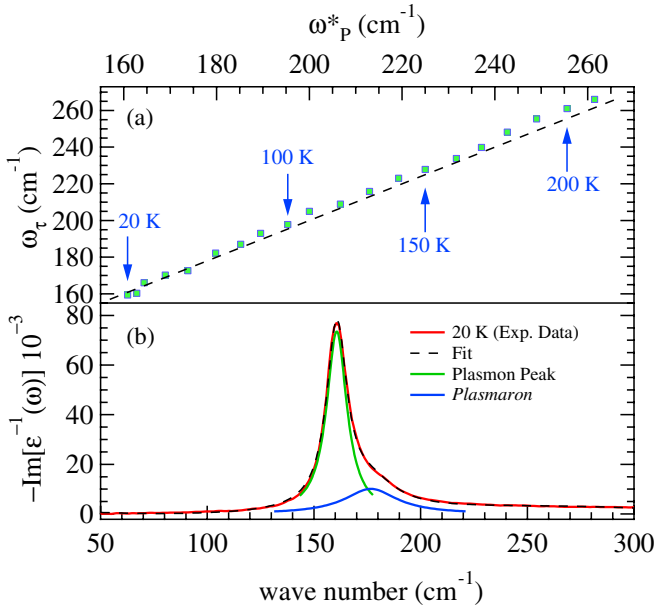

FIG. 4 (color online). (a) A parametric plot ω_τ vs ω_p^* shows a slope of 1 supporting the hypothesis of an electron-plasmon interaction. (b) The 20 K loss function presents the main plasmon peak and a *plasmaron* peak appearing as a shoulder of the main one.

agreement only by considering an exceptionally large charged impurity concentration ($N = 1.5 \times 10^{19}$ cm^{-3}). This is approximately 2 orders of magnitude greater than the carrier concentration itself and implies a *charged* impurity concentration of 1 part in 10^4, which we consider to be unrealistic considering the high purity of our samples.

In contrast, we propose that we are observing the excitation of plasmons via a decay channel of the electron-hole pairs. This interaction should be similar to that considered in the context of electron—phonon [22] or electron—magnon scattering [23]. Such an interaction has been theoretically anticipated. It may be captured within the same Holstein Hamiltonian that is used to treat the electron—longitudinal phonon coupling and describe polarons, and so this collective excitation has been called a *plasmaron* [24,25]. Such an excitation is only possible optically in a system where translational symmetry has been broken first by, for instance, Umklapp scattering or disorder that moves oscillator strength to a frequency region near the plasmon energy. In normal metals, such an interaction is completely unobservable as the plasmon energy scales are many orders of magnitude higher than transport ones. This is, to the best of our knowledge, the first unambiguous observation of conduction band scattering with a collective bosonic mode of purely electronic origin.

Our results have some relation to the classic observation of plasmon excitation in electron energy loss experiments [26], as this is also an electron-plasmon coupling. However, in that classic case, the coupling of electrons to plasmons is at such high energies that it is essentially irrelevant to the low energy properties of the material. Our observation is direct evidence for a coupling of low energy conduction band electrons to plasmons. This coupling will have a direct effect on the transport and other properties of the material, just like electron-phonon or magnetic couplings may. This observation is made possible in Bi by its low temperature dependent carrier density, a very large ϵ_∞, and a lack of optically active phonons.

Within the electron-hole plasmon decay channel scenario, one might try to model the scattering rate using an expression for the plasmon density of states $D(\omega)$ and a simple scheme for coupling of the spectrum to electronic excitations [22,23]. Unfortunately, in the present case, such a calculation is hard to compare with the data exactly, due to the onset of interband contribution. Moreover, the low energy prepeak structure is interesting and is *not* captured within any such simple models. A complementary view of it can come from the loss function $\mathrm{Im}\{-\varepsilon^{-1}(\omega)\}$, shown in Fig. 4(b) for $T = 20$ K, which reveals a two-peak structure, one centered at the screened plasma frequency $\omega_p^* = 160.7$ cm^{-1} with a width $\gamma_1 = 5.74$ cm^{-1} and a weaker one at $\omega_2 = 176.4$ cm^{-1} with $\gamma_2 = 15.6$ cm^{-1}. The position of this latter peak corresponds exactly to the position of the absorption feature seen in $\varepsilon_2(\omega)$ thus demonstrating its admixture of longitudinal plasmon character.

In conclusion, we have reported the optical signatures of conduction electrons coupled to plasmons, i.e., plasmarons, in pure Bi. It is possible that reducing the charge density further, perhaps through the application of pressure, may enhance such interactions and drive the system into an anomalous metallic state. Pressure dependent optical studies may prove to be a useful probe in this regard. It would also be interesting to search for similar effects in other semimetals like graphite or single-layer graphene.

We gratefully acknowledge F. Carbone, M. Dressel, H. D. Drew, A Kuzmenko, and A. J. Millis for helpful discussions. This work is supported by the Swiss National Science Foundation through Grant No. 200020-113293 and the NCCR-MaNEP. N. P. A. has been supported by the US NSF.

[1] N. B. Brandt *et al.*, Sov. Phys. JETP **20**, 301 (1965).
[2] D. Balla and N. B. Brandt, Sov. Phys. JETP **20**, 1111 (1965).
[3] V. S. Édel'man, Adv. Phys. **25**, 555 (1976).
[4] X. Du, S. W. Tsai, D. L. Maslov, and A. F. Hebard, Phys. Rev. Lett. **94**, 166601 (2005).
[5] Y. Kopelevich *et al.*, Phys. Rev. B **73**, 165128 (2006).
[6] K. S. Novoselov *et al.*, Nature (London) **438**, 197 (2005).
[7] Y. Zhang *et al.*, Nature (London) **438**, 201 (2005).
[8] Y. F. Komnik *et al.*, Sov. Phys. JETP **33**, 364 (1971).
[9] F. Y. Yang *et al.*, Science **284**, 1335 (1999).
[10] B. K. Chong *et al.*, J. Vac. Sci. Technol. A **19**, 1769 (2001).
[11] K. I. Lee *et al.*, Phys. Status Solidi B **241**, 1510 (2004).
[12] G. Mahan, *Many Particle Physics* (Kluwer Academic, New York, 2000), 3rd ed..
[13] J. Heremans and O. P. Hansen, J. Phys. C **16**, 4623 (1983).
[14] A. B. Kuzmenko, Rev. Sci. Instrum. **76**, 083108 (2005).
[15] W. S. Boyle and A. D. Brailsford, Phys. Rev. **120**, 1943 (1960).
[16] J. W. Allen and J. C. Mikkelsen, Phys. Rev. B **15**, 2952 (1977).
[17] M. P. Vecchi and M. S. Dresselhaus, Phys. Rev. B **10**, 771 (1974).
[18] E. Gerlach and M. Rautenberg, Phys. Status Solidi B **65**, K13 (1974).
[19] E. Gerlach *et al.*, Phys. Status Solidi B **75**, 553 (1976).
[20] L. M. Claessen, A. G. M. Jansen, and P. Wyder, Phys. Rev. B **33**, 7947 (1986).
[21] J. Mycielski and A. Mycielski, Phys. Rev. B **18**, 1859 (1978).
[22] F. Marsiglio, J. P. Carbotte, and E. Schachinger, Phys. Rev. B **65**, 014515 (2001).
[23] J. Carbotte, E. Schachinger, and D. N. Basov, Nature (London) **401**, 354 (1999).
[24] B. Lundqvist, Phys. Kondens. Mater. **6**, 193 (1967).
[25] B. Lundqvist, Phys. Status Solidi **32**, 273 (1969).
[26] C. J. Powell and J. B. Swan, Phys. Rev. **115**, 869 (1959).